Dextran mass ratio controls particle drying dynamics in a thermally stable dry powder vaccine for pulmonary delivery

Myla Manser[a], Blair A. Morgan[a], Xueya Feng[b], Rod G. Rhem[c], Myrna B. Dolovich[c], Zhou Xing[b], Emily D. Cranston[a,d,e], Michael R. Thompson[a,*]

[a] Department of Chemical Engineering, McMaster University, Hamilton, Ontario, L8S 4L7, Canada

[b] McMaster Immunology Research Centre and Department of Pathology and Molecular Medicine, McMaster University, Hamilton, Ontario, L8S 4L7, Canada

[c] Firestone Research Aerosol Laboratory, St. Joseph's Healthcare and Department of Medicine, McMaster University and Hamilton, Ontario, L8N 4A6

[d] Department of Wood Science, University of British Columbia, 2424 Main Mall, Vancouver, BC, V6T 1Z4, Canada

[e] Department of Chemical and Biological Engineering, University of British Columbia, 2360 East Mall, Vancouver, British Columbia, V6T 1Z3, Canada

[*]Corresponding author: Michael Thompson, mthomps@mcmaster.ca

Key Words

Spray Drying; Dextran; Thermal Stability; Inhalation; Drying Dynamics

Abstract

Purpose: Thermally stable, spray dried vaccines targeting respiratory diseases are promising candidates for pulmonary delivery, requiring careful excipient formulation to effectively encapsulate and protect labile biologics. This study investigates the impact of dextran mass ratio and molecular weight on activity retention, thermal stability and aerosol behaviour of a labile adenoviral vector (AdHu5) encapsulated within a spray dried mannitol-dextran blend.

Methods: Comparing formulations using 40 kDa or 500 kDa dextran at mass ratios of 1:3 and 3:1 mannitol to dextran, *in vitro* quantification of activity losses and powder flowability was used to assess suitability for inhalation.

Results: Incorporating mannitol in a 1:3 ratio with 500 kDa dextran reduced viral titre processing losses below 0.5 log and displayed strong thermal stability under accelerated aging conditions. Moisture absorption and agglomeration was higher in dextran-rich formulations, but under low humidity the 1:3 ratio with 500 kDa dextran powder had the lowest mass median aerodynamic diameter (4.4 μm) and 84% emitted dose from an intratracheal dosator, indicating strong aerosol performance.

Conclusions: Overall, dextran-rich formulations increased viscosity during drying which slowed self-diffusion and favorably hindered viral partitioning at the particle surface. Reducing mannitol content also minimized AdHu5 exclusion from crystalline regions that can force the vector to air-solid interfaces where deactivation occurs. Although increased dextran molecular weight improved activity retention at the 1:3 ratio, it was less influential than the ratio parameter. Improving encapsulation ultimately allows inhalable vaccines to be prepared at higher potency, requiring less powder mass per inhaled dose and higher delivery efficiency.

1. Introduction

Vaccine thermal sensitivity is one of the largest hurdles currently facing global immunization efforts. In low-income countries, particularly those with tropical or semi-arid climates, access to the necessary cold-chain infrastructure is limited and incredibly expensive. The resulting immunization programs in these regions suffer from insufficient storage capacity and cold-chain equipment failure, leading to vaccine wastage or reduced vaccine potency due to poor temperature control (1,2). To reduce this geographical discrepancy and improve global vaccine access,

development efforts have started using processing methods such as spray drying to achieve thermal stability of active vaccine components in dry powder form (3,4,5,6,7).

Thermal stabilization of a spray dried biologic is based upon the *water replacement hypothesis*, where its proteins favorably interact with the hydroxyl groups of excipients like carbohydrates to retain the native protein structure and prevent denaturation (8). Careful excipient formulation is a critical aspect in the successful encapsulation of highly labile biologics such as adenoviruses (9). Although recombinant adenoviral (Ad) vectors such as human serotype 5 Ad vector (AdHu5) have been utilized to develop human vaccines against respiratory infectious diseases including COVID-19 (10) and tuberculosis (11), they are particularly labile at elevated temperatures and prone to structural damage (12,13). This functional limitation highlights the value of developing a thermally stable, dry powder preparation for pulmonary delivery of Ad-vectored vaccines, with the goal of maintaining stability for several months at room temperature.

A blend of mannitol and dextran has been previously shown to successfully retain viral activity of AdHu5 through spray drying, in addition to providing thermal stabilization (9,14,15). Of these previous studies, the most successful formulation blended mannitol and dextran in a 3:1 mass ratio using a moderately low molecular weight dextran of 40 kDa (16). Within this blend, dextran acts as the major amorphous component known to effectively stabilize the matrix through vitrification (14).

During particle drying dextran diffuses slowly and increases the viscosity of the solution, while encouraging surface-active components mannitol and AdHu5 to diffuse towards the droplet center away from the air-liquid interface and dextran-rich particle surface (17,18). By preventing viral partitioning at the air-solid particle interface, dextran can effectively shield the adenovirus from the high heat environment in the drying chamber of the spray dryer. Once the particle is dry,

dextran helps to minimize adenovirus mobility within the matrix to prevent viral aggregation, which is a known cause of viral deactivation and activity loss (19). Dextran exhibits a relatively high glass transition temperature (T_g) making it a preferred choice for encapsulating and stabilizing an adenovirus at elevated temperatures (9). However, dextran alone does not show good water replacement characteristics with the adenovirus resulting in high activity losses (9). As a hygroscopic amorphous solid, dextran is moisture sensitive under elevated humidity conditions leaving it susceptible to T_g depression (20).

Comparatively, mannitol is much smaller than a dextran polymer and more readily forms hydrogen bonds with the protein capsid of the adenovirus which can prevent denaturation (9). Although mannitol interacts strongly with the protein capsid layer of an adenovirus, anchoring it within the particle matrix during particle drying, it also has the tendency to crystallize. Crystalline regions formed by this sugar impede moisture absorption and are associated with lower surface energy and increased thermodynamic stability of produced dry powders (21). However, these crystalline regions can also lead to viral exclusion which limits the extent of viral encapsulation (17,22). Fine particle crystalline materials are also known to experience high inter-particulate cohesion, leading to poor dissolution and reduced absorption efficiency in the lungs upon inhalation (21,22). Particle cohesion also reduces aerosolization and must therefore be controlled. We hypothesize that our previously identified mannitol-dextran excipient blend could be further improved by reducing the relative amount of mannitol within the blend. This would reduce the negative impact of crystal formation within an inhalable product and allow the adenovirus to remain fully encapsulated within the interior of the particle, minimizing viral deactivation in an inhalable spray dried vaccine. This study investigates the role of molecular weight and mass ratio

of dextran on the retained activity, thermal stability and powder flowability of a spray dried AdHu5 adenoviral vector intended for pulmonary dry powder delivery.

2. Materials & Methods

2.1 Chemical and Biologics

D-mannitol, xylitol and dextran (M_r 40000 Da) were all sourced from Millipore-Sigma (ON, Canada) as USP grades. High molecular weight dextran (M_r 500000 Da) was purchased from ThermoFisher Scientific (Waltham, MA, USA). Milli-Q® water was purified with a Barnstead GenPure Pro system from ThermoFisher Scientific (Waltham, MA, USA) using a resistivity of 18.2 MΩ cm. A-549 epithelial lung tumor cells were used for all cell culturing experiments and were grown in a culture media described in a Life Technologies protocol from Invitrogen (ON, Canada) which consisted of α-minimum essential media (α-MEM) mixed with 1% streptomycin/penicillin and 10% fetal bovine serum (FBS). A recombinant human serotype 5 adenovirus expressing Green Fluorescent Protein (AdHu5) was prepared in the McMaster University Immunology Research Centre vector facility and was modified to be replication deficient. Upon purification, the adenoviral vector stock was stored in a 5% trehalose storage buffer at -80 ºC and had a titre of 4.4×10^8 pfu/mL (15).

2.2 Modelling Excipient Distribution in Spray Dried Particles

A diffusion-based single droplet drying model developed and validated by Morgan et al. (17) was used to predict the distribution of dextran and AdHu5 within a dry particle for each of the mannitol-dextran blends using MATLAB (Mathworks, Inc; Natick, MA, USA). Although the model was validated based on acoustically levitated particles with radii on the scale of 200 µm, it has been previously demonstrated that acoustic levitation and spray drying can produce particles

with similar morphologies, thermal properties and viral activity trends due to comparable drying kinetics (23). Therefore, we expect that this model is an appropriate approximation for excipient diffusion and the relative component distribution experienced during spray drying. Component distribution was plotted across the radius of a drying particle by dividing the particle into 40 shells spanning the radial axis. The weight fraction of each component at a specific shell is reported as a mass%, normalized based on the total amount of that specific component added to the excipient blend.

2.3 Sample Preparation and Spray Drying

Excipient solutions were prepared using a mannitol-to-dextran (MD) mass ratio of either 3:1 or 1:3 by dissolving excipients in purified Milli-Q® water to a concentration of 1% solids. Either low molecular weight dextran (40 kDa) or high molecular weight dextran (500 kDa) was used to prepare each formulation ratio. For comparison, a xylitol-dextran formulation was also prepared at a 1:3 ratio using 40 kDa dextran. Details and corresponding notations for all five excipient formulations are summarized in Table 1. A volume of 60 µL AdHu5 stock vector with 5% trehalose was added per 100 mg of excipient based on our previous work that improved viral activity retention at high loading via appropriate selection of the cryoprotective storage solution (15). In all physical characterization and flowability tests described in Section 2.6, a placebo solution of 5% trehalose was added at 60 µL/100 mg of excipient instead of the viral stock, as particle size and morphology of mannitol-dextran spray dried powder is the same with and without AdHu5 present (16).

Once the excipients were fully dissolved in solution, spray dried powders were produced using a a B-290 Mini Spray Dryer from Büchi (Switzerland) outfitted with a 0.7 mm nozzle. It should be noted that excipient solutions with 500 kDa dextran were refrigerated at 4 °C for at least

30 minutes to achieve full dissolution prior to spray drying. For accurate comparison between each excipient formulations, all spray dryer settings were kept consistent for each batch. Based on previous process optimization of yield, particle size and viral activity (16), the following settings were used: 120 ºC inlet temperature, 217.5 mL/h feed flow rate (pump setting 13%), 439.11 L/min spray gas flow rate (30 mm rotameter reading) and 35 m/h aspirator flow rate (100% aspiration). The outlet temperature ranged between 55-65 ºC. Immediately after drying, powder was collected into microcentrifuge tubes within a biosafety cabinet and transferred to a benchtop desiccator for storage at room temperature on Drierite® anhydrous indicating desiccant (W.A Hammond Drierite Company Ltd.). Powders were transported between lab spaces using a vacuum sealed storage container that contained additional desiccant to avoid exposure to ambient humidity.

2.4 Cell Culturing

Stock suspension of A-549 cells was stored in liquid nitrogen under cryo-storage conditions. Once thawed, cells were added to pre-warmed α-MEM and centrifuged for 5 minutes at 1400 rpm to obtain a cell pellet. A single cell suspension was prepared by resuspending the pellet in α-MEM and plating in a T-150 flask for overnight incubation at 37 ºC and 5% CO_2 in a water jacketed incubator (Forma Scientific Inc., Marietta, OH, USA). Dead cells and remaining dimethyl sulfoxide from cryo-storage were removed the following day by exchanging cell media and passaging the confluent culture twice before *in vitro* testing on a 96-well plate.

2.5 Viral Activity Testing via Flowcytometry

Viral activity testing of each spray dried powder formulation was tested *in vitro* by following the same protocol described in our previous work (15). Briefly, α-MEM was used to reconstitute each spray dried sample to a solids concentration of 1% immediately before infecting

40,000 confluent A-549 cells on a 96-well plate and incubating overnight at 37 ºC. Cell washing, trypsinization and fixation with 1% paraformaldehyde was performed prior to flowcytometry analysis with a Beckman Coulter Life Sciences CytoFlex LX flow cytometer (Indianapolis, IN, USA). At least 10,000 events were analyzed per sample to account for 25% of the plated cell population using CytExpert software. FlowJo® software (BD, New Jersey, USA) was used to quantify GFP expression within the live cell population, excluding cellular debris and artifacts using the auto-gating tool. A calibration curve was used to convert GFP expression to viral multiplicity of infection (MOI). Viral titre was then calculated based on the MOI and normalized based on sample mass of the spray dried powder. Processing losses in viral titre due to spray drying are discussed on the log scale via viral titre log loss.

2.6 Thermal Aging

Each spray dried formulation was stored under accelerated aging conditions to determine the impact of excipient formulation on thermal stability of the encapsulated adenovirus. Using a previously described protocol (15), each powder formulation was stored in a water bath at 45 ºC for 72 hours prior to GFP quantification via flowcytometry. Moisture uptake was prevented during the aging process by storing the spray dried powder within microcentrifuge tubes that were sealed with Parafilm® wax, placed within a plastic bag containing desiccant and added to a sealed glass jar with additional desiccant. Immediately after the 72-hour aging process, samples were removed from the water bath and resuspended in α-MEM for cell infection and viral activity tested as in Section 2.5. Viral activity for all aged samples was tested in duplicate and error bars represent the standard error between samples.

2.7 Particle Flowability and Characterization

2.7.1 Moisture Content via Thermogravimetric Analysis

Thermogravimetric analysis (TGA) was used to determine total moisture content in each spray dried powder formulation following processing and thermal aging. Moisture analysis was conducted on samples stored under accelerated aging conditions at 45 ºC for 72 hours. Between 5-10 mg of sample was loaded into an alumina crucible and heated in a TGA/DSC 3+ LF/1100 instrument from Mettler Toledo (Columbus, Ohio, USA) at a rate of 5 ºC/min until reaching 150 ºC where the temperature was held constant for 10 minutes under argon gas. Mass was monitored over the tested temperature range using STARe software from Mettler Toledo (Columbus, Ohio, USA). Moisture content was determined based on the percentage of mass change from 25 ºC to approximately 110 ºC, when the sample mass had stabilized. Standard error was determined based on duplicate sample measurement.

2.7.2 Scanning Electron Microscopy (SEM)

A Tescan Vega II LSU scanning electron microscope (Tescan Orsay Holding, a.s., Brno, Czech Republic) was used for qualitative analysis of the spray dried particle morphology. To prepare samples for imaging, a Polaron E5100 sputter coater (Quorum Technologies Limited, Laughton, UK) was used to coat a 24 nm layer of gold on top of sample secured by double-sided carbon tape. An electron accelerating voltage of 20 kV and magnification of 2000 were used to capture micrographs at a working distance range between 10.12 - 10.14 mm.

2.7.3 Geometric Particle Sizing

Geometric particle sizing was conducted with a Helos R-series laser diffraction sensor from Sympatec GmbH (Pulverhaus, Germany) using an R2 lens with a 50 mm focal length for a reliable detection range between 0.45 – 87.5 μm in size. Powder samples with mass weighed between 7-12 mg were loaded into and dispensed from an ICOone™ inhaler provided generously by Iconovo (Lund, Sweden). The ICOone™ inhaler is designed for single-dose usage with medium resistance and fabricated as one piece via injection molding, making it a suitable device for administering vaccines through inhalation (24). Aluminum foil is intended to protect the powder formulation within the device, however protective foil was not used in this study. A cumulative particle size distribution was generated, with median particle diameter represented by the 50th percentile (D50) of the distribution. Span of the particle size distribution was determined with the values of the 10th (D10), 50th and 90th (D90) percentiles based on Eq 1. All samples were measured in duplicate and error bars represent standard error between samples.

$$Span = \frac{D90 - D10}{D50} \quad (1)$$

2.7.4 Aerodynamic Particle Size

Aerodynamic particle size distribution was experimentally determined using a Next Generation Impactor (NGI) from Copley Scientific Limited (Nottingham, UK). Filter paper was used to line each of the impactor stages for gravimetric analysis of particle mass deposition. Five ICOone™ inhalers were loaded with 8-12 mg of spray dried powder, for a total nominal dose of approximately 50 mg, and immediately dispersed into the impactor drawing a flow rate of 60

L/min. Total air volume drawn per sample was approximately 100 L. Dry powder inhalers were tested with a pressure drop of 4 kPa across each device, with calibrated pressure drop across the assembled NGI being approximately 10 kPa. The mass median aerodynamic diameter (MMAD) was calculated based on the cumulative particle size distribution from gravimetric measurements.

2.7.5 Bulk Density, Tapped Density and Carr's Index

Bulk density of spray dried powder was determined using a method loosely based on a scaled down USP protocol for powder bulk density measurement published in the International Pharmacopoeia (25). By pouring a known mass of powder into a graduated cylinder with minimal agitation, the volume was recorded and used to determine bulk density. Although the USP protocol for bulk density testing in the European pharmacopeia states that a scaled down test can utilize a 25 mL graduated cylinder for bulk volume measurement, this would still require powder mass in quantities far larger than feasibly produced with the lab scale spray dryer. Hughes et al. have shown that a material sparing testing method for bulk density using a 10 mL cylinder produced acceptable results comparable to the USP method (26). Here, the bulk density testing method was further scaled down to a 1 mL graduated cylinder, readable to 0.1 mL, using 200 mg of powder per measurement to save needing additional material.

Tapped density was determined by manually tapping a syringe filled with approximately 200 mg of powder for 1 minute at a rate of 2 taps/s. Tapping height was approximately 2 cm. The powder mass was divided by the difference between recorded volume before and after tapping to determine tapped density. As an indicator of powder flowability, the percentage of powder compressibility (Carr's Index) was calculated based on Eq. 2. Prior to data collection, the experimental method was validated based on a standard Carr's Index scale for flowability. Further details on experimental set-up and method validation can be found in Figure S1 and Table S1 of

the Supplementary Material. All spray dried powder formulations were tested in triplicate using the described method and error bars represent standard error between measurements.

$$Carr's\ Index = \frac{\rho_{tapped} - \rho_{bulk}}{\rho_{tapped}} \quad (2)$$

2.7.6 Intratracheal Delivery Device (Dosator)

An intratracheal dosator device intended for *in vivo* testing with a murine animal model was assembled based on similar custom designs described by Ihara et al. and Qui et al. which both used a 3-way stopcock to control airflow from a syringe through a gel-loading pipette or needle tip (27,28). Briefly, our intratracheal dosator consisted of a 1 mL syringe with a male luer lock connection that twists onto a complementary luer inlet on a 3-way stopcock purchased from Cole-Parmer (Montreal, Canada). An air volume of 0.6 mL was pre-drawn in the syringe prior to securing the luer lock connection. Between 3-4 mg of powder was weighed onto weigh paper and carefully poured into a 10 µL Rainin LiteTouch System pipette tip (Mettler-Toledo, Oakland, CA, USA) before tightly fastening the pipette tip on the opposite end of the 3-way stopcock. After ensuring the valve was correctly oriented, powder was dispersed through the tip by quickly depressing a pre-drawn syringe. A new pipette tip with freshly loaded powder was used when each sample was sprayed. Individual components of the intratracheal dosator, as well as the final assembly loaded with powder, can be visualized in Figure 1.

2.7.7 Emitted and Delivered Dose

To test the functionality of this intratracheal dosator and compatibility with each spray dried powder formulation, powder was loaded into the dosator and released through a 3D printed model of a mouse trachea and into a glass collection vial (Figure 1). The 3D trachea model was

developed using CT scans from mice, which were converted into binary images in MATLAB (Mathworks, Inc; Natick, MA, USA) and used to produce a CAD rendering. To improve the durability, the wall thickness of the printed trachea was increased to 2.5 mm while keeping the internal geometry printed to scale. See Figure S2-S7 in Supplementary Material for further details. The 3D trachea was printed with a ProJet® MJP 2500 Plus from 3D Systems (South Carolina, USA) using the ultra high-definition printing mode with VisiJet M2R-CL rigid plastic (3D Systems, South Carolina, USA). Figure 1 (panel C) shows the experimental set up used for device testing. The dosator was tested in a vertical orientation for all measurements to closely represent the needle positioning used during *in vivo* intratracheal delivery of dry powder to mice. This orientation also minimized any variation during repeated device set-up and actuation. A retort stand with clamp was used to secure the dosator assembly above the collection vial for consistency between actuations. Emitted dose from the intratracheal dosator was determined after loading the tip with a known mass of powder and measuring the mass of the dosator assembly before and immediately after actuation. This difference was divided by the total powder loaded in the tip and expressed in terms of percentage, as indicated in Eq. 3. The calculated emitted dose accounted for all powder losses within the pipette tip and at the luer lock connection point. Triplicate measurements were performed, with error bars representing the standard error.

$$Emitted\ Dose = \frac{Dosator\ Mass_{Before} - Dosator\ Mass_{After}}{Powder\ Loaded} \times 100\% \quad (3)$$

To approximate the amount of powder that could be effectively delivered through a mouse trachea and into the lungs, the tip of the intratracheal dosator was sprayed directly into the 3D printed mouse trachea. The other end of the trachea was secured on top of a glass collection vial. By measuring the mass of the collection vial before and after powder administration from the dosator, delivered dose was calculated (Eq. 4). In this context, the delivered dose refers to the

percentage of powder that successfully flows through the 3D printed mouse trachea for delivery into the lungs with respect to total powder loaded. All measurements were performed in triplicate, with error bars representing standard error.

$$Delivered\ Dose = \frac{Vial\ Mass_{After} - Vial\ Mass_{Before}}{Powder\ Loaded} \times 100\% \quad (4)$$

3. Results & Discussion

3.1 Predicted Component Distribution in Spray Dried Particles

We used our previously established mannitol-dextran formulation, MD (3:1) with 40 kDa dextran, as a baseline to compare the impacts of increasing the relative dextran content and molecular weight of dextran. Using a diffusion-based drying droplet model, the relative distribution of AdHu5 was predicted with respect to the radial distance to the particle surface (Figure 2). The displayed AdHu5 mass% was normalized by the total concentration of AdHu5 added to the excipient blend, not the total mass of all excipient components. It should be noted that the particle was treated as a series of finite thick shells to predict the distribution of components throughout.

Based on the model output, the baseline formulation of MD (3:1)-40 kDa led to the highest amount of adenovirus located at the particle surface and had the lowest predicted amount of adenovirus throughout the solid inner layers of the particle. In comparison, the formulation with lowest predicted adenovirus on the particle surface was MD (1:3)-500 kDa. The molecular weight of dextran was predicted to significantly influence adenovirus surface concentration, as both

formulations containing 500 kDa dextran showed lower AdHu5 mass% on the particle surface compared to the 40 kDa counterparts. A similar prediction was previously reported with this model for levitated particles and was verified experimentally with fluorescently tagged-protein coated silica nanoparticles as adenovirus analogues (17). Using atomic force microscopy and confocal laser microscopy, the previous study identified the relative location of adenovirus analogues within dried particles to validate the model prediction that excipient formulation can influence surface concentration and partitioning of AdHu5 (17). Similarly, uniform dispersion of AdHu5 throughout the particle was not observed in the model predictions of the current study which indicates that AdHu5 became encapsulated during the drying process.

Higher molecular weight dextran at a higher concentration experiences much slower self-diffusion of dextran entanglements and creates an obstruction effect on the smaller solutes within the droplet (29,30). With dextran acting as a physical obstacle, diffusion of mannitol and AdHu5 within the bulk droplet is hindered and may explain why AdHu5 is less likely to partition on the particle surface. Previous reports have noted that increased viral concentration on or near the surface of a drying particle can lead to reduced viral activity (14,17). Consequently, we anticipate that vaccine formulations with lower predicted viral mass at the surface are likely more effective at retaining biologic activity under experimental conditions.

Furthermore, both formulations containing a 1:3 ratio of mannitol-to-dextran had a higher predicted mass% of AdHu5 at the particle core compared to the formulations using a 3:1 ratio. These 1:3 formulations also have a more uniform distribution of dextran throughout the particle, in contrast to the dextran-enriched particle surface seen for 3:1 formulations. Dextran has a substantially larger impact on viscosity, compared to mannitol and AdHu5, resulting in a much lower diffusion coefficient in water (31). This effect is particularly relevant in the 3:1 formulations,

as dextran becomes enriched on the droplet surface during solvent evaporation where it reaches saturation and precipitates (17). Since increasing dextran concentration in water has been found to increase the solution viscosity (32), incorporating more dextran within the formulation physically prevented mannitol from diffusing towards the droplet surface. As a result, mannitol can closely interact with AdHu5 in the particle core to provide stabilization though hydrogen bonding. It should also be noted that encapsulating AdHu5 in 40 kDa dextran alone has been experimentally shown to yield poor viral activity, likely due to the inability of dextran to effectively stabilize AdHu5 through water-replacement hydrogen bonding (9). Overall, these model predictions suggest that the formulation with higher molecular weight and mass ratio of dextran favors more viral entrapment at the particle core, which should be verifiable by activity testing.

3.2 Viral Activity and Thermal Aging

To validate the model predictions, viral activity was experimentally tested immediately after spray drying as well as after accelerated thermal aging for each powder formulation (Figure 3). Here we compare results to a xylitol-dextran blend where, xylitol is chemically similar to the structure of mannitol and has previously been shown to retain high viral activity through spray drying (23). In terms of activity losses attributed to processing, minimal viral titre log losses were observed immediately after spray drying when a 1:3 ratio was used for either mannitol or xylitol blends. Processing loss for the MD (1:3)-500 kDa and XD (1:3)-40 kDa were both below the acceptable threshold of 0.5 log loss, indicating very favorable results. The MD (1:3)-40 kDa was slightly above the target threshold with viral titre log losses that were slightly below 0.8 log loss. Processing losses were significantly higher for the powders formulated with a 3:1 mannitol-to-dextran ratio, exceeding 1.7 log loss. These results generally reflect the model prediction, in that viral activity was the highest for the MD (1:3)-500 kDa formulation with the lowest amount of

AdHu5 predicted at the air-particle interface. Likewise, MD (3:1)-40 kDa had the highest predicted AdHu5 at the air-particle interface and had low viral activity after processing. A slight deviation between modelled distributions and experimental activity was observed in the MD (3:1)-500 kDa, giving the highest overall activity loss. However, the model does not currently account for crystallinity or void formation within dry particles, which may have contributed to the different experimental outcome. It should be noted that formal process optimization was only conducted for the baseline MD (3:1)-40 kDa formulation, as the process yield was similar for all other mannitol-dextran formulations (data not shown). Since yield can be an indicator of spray drying process efficiency, this suggested that additional optimization of processing parameters was not necessary for the purposes of this study.

Despite their valued role in hydrogen bond stabilization, mannitol and xylitol both added some crystallinity to the overall particle matrix which can negatively impact viral activity. Previously reported x-ray diffraction (XRD) data has shown that spray dried particles consisting only of dextran did not display any crystalline peaks, while spray dried mannitol-dextran particles in a 3:1 ratio exhibited crystalline behaviour resembling the α-polymorphic form of mannitol (14). Furthermore, our group previously reported that the molecular weight of dextran does not change the overall crystallinity of acoustically levitated mannitol-dextran particles (17), which supports that the mass ratio of mannitol or xylitol controls the extent of crystallinity within the dry powder. Incorporating a lower mass of xylitol or mannitol minimizes crystal exclusion of the adenovirus within particles that would otherwise force the biologic towards an air-particle boundary or potentially even damage the structural integrity of the virus (17). If the adenovirus is located on the particle surface or any air-solid boundary, there is a greater chance of exposure to high heat during processing and higher activity losses (13,14,16,17). Additionally, including a higher

fraction of dextran promotes stronger thermal shielding upon exposure to the outlet temperature conditions to protect against structural degradation of the protein capsid for better activity retention (13). Since the molecular weight of dextran does not impact crystallinity, its impact on AdHu5 partitioning within the particle is diffusion controlled. Using a higher molecular weight dextran may further increase viscosity during drying (32), impeding molecular movement of the adenovirus that might otherwise lead to viral aggregation. However, at the 3:1 ratio, the 500 kDa dextran led to a slightly higher viral titre log loss than the 40 kDa formulation, suggesting that the molecular weight of dextran was less influential on viscosity than its concentration in the droplet.

Thermal stability was also tested in all five formulations, by analyzing viral activity retention upon exposure to accelerated aging conditions at 45 ºC for 72 hours. All mannitol-dextran formulations display similar thermal aging behaviour, based on aging losses being of similar magnitude for each of these formulations (Figure 3). This suggests that there were no significant differences in T_g between these formulations. This observation is directly supported by T_g values reported in literature, which indicate that 40 kDa and 500 kDa dextran have a T_g of approximately 223 ºC and 225 ºC, respectively (33). Measured T_g values are often associated with an error range of 10 ºC, depending on the method of measurement (44,45), indicating that a 2º C difference in Tg between 40 kDa and 500 kDa dextran is not highly significant. Mannitol-dextran formulations showed superior thermal stability, compared to the xylitol-dextran blend which experienced 1.1 log loss during thermal aging.

Notably, the combined processing and aging losses experienced by the MD (1:3)-500 kDa formulation were below 0.8 log loss. The chemical structure of xylitol and mannitol is very similar, differing only by one C-OH group. But as an individual sugar alcohol, amorphous xylitol has a very low T_g of -24 ºC and will readily recrystallize at room temperature (34). Comparatively, the

reported T_g of amorphous mannitol is around 12 °C (35), which significantly improves the overall T_g in a dextran blend compared to xylitol. Under elevated thermal conditions, the xylitol-dextran blend likely experienced a higher degree of molecular mobility that led to viral aggregation. Xylitol recrystallization may have also forced more adenovirus towards the air-particle interfaces where thermal stresses during aging could have caused deactivation. Similarly, reorganization of the excipient crystal structure could have resulted in structural rearrangement and denaturation of the adenovirus causing poor stability (36). Due to the significantly higher thermal aging losses observed with the use of xylitol, this formulation was considered to have poor thermal stability and was not used for further characterization. Despite past reports indicating xylitol as a promising excipient for vaccine powders (23), to the best of our knowledge this is the first study showing that the thermal aging properties of xylitol in blended systems are likely unsuitable to protect viral vectors during vaccine storage and distribution.

The accelerated aging conditions used in this study are routinely used to assess the stability of vaccine formulations, often used to identify excipient candidates that may achieve or exceed the desired stability criteria (46). Although accelerated studies are an efficient screening tool, long-term studies are still required to accurately determine the shelf-life of an inhalable dry powder formulation.

3.3 Moisture Content and Particle Morphology

Since excessive water uptake can hinder dry powder stability, TGA was used to measure moisture content in each mannitol-dextran formulation after exposure to accelerated aging conditions (see Table 2). Moisture content for the MD (1:3)-40 kDa formulation was 4.6%, which

was slightly higher than the remaining mannitol-dextran formulations that contained closer to 3% moisture. Since moisture content was measured after 72 hours of thermal aging, these values indicate that formulations with a greater concentration of dextran had a higher capacity for moisture absorption under elevated storage temperatures. Kawaizumi et al. found that dextran hydration decreases with increasing molecular weight (20), which could explain why MD (1:3)-500 kDa did not have the same moisture content as the MD (1:3)-40 kDa formulation. As such, using a higher molecular weight dextran may also promote more effective, long-term stabilization of the encapsulated adenovirus.

Powder morphology of each mannitol-dextran formulation was observed by SEM (Figure 4). Formulations with a 1:3 mannitol-dextran ratio appeared to be highly clumped with large agglomerates observed, also indicating higher moisture content and stickiness in these powders. Handling and preparation of these powders was conducted in a lab space with increased ambient humidity directly before particle imaging, so the observed agglomeration may be further indication that increased amorphous content causes an increased capacity for moisture absorption. These particles appeared to have a rough outer surface, but solid particle structure. Agglomeration and clumping due to liquid bridge formation appears to be worse in the MD (1:3)-40 kDa sample, compared to the same ratio with 500 kDa. This qualitative observation is in direct agreement with the measured moisture content and may also be attributed to the natural tendency of hydrophilic polymers to experience “stickiness” in the presence of water. Dextran is a hygroscopic material (20), so a higher amorphous content increased the capacity for moisture absorption when exposed to humidity.

Comparatively, formulations that contained more mannitol appeared to have a smoother particle surface, with the tendency to form hollow shells (as evidenced by the dimpling and

rounded indentation observed in Figures 4C and 4D). Hollow shell formation is indicative of particles with a high *Peclet* number, in which evaporation occurs faster than solute diffusion (32). Clumping is also less evident in the samples with higher crystalline content. Moisture absorption can ultimately reduce the T_g of the formulation through a plasticization effect, leading to reduced thermal stability and poor viral activity retention over time (37). Therefore, protocols for handling spray dried powders with high amorphous content and some degree of crystallinity must minimize exposure to humidity as much as possible (i.e., through the use of double-wrapped powder blister packs and/or desiccants during storage).

3.4 Geometric and Aerodynamic Particle Size

To assess the suitability of these powders for inhalation, both geometric particle size and aerodynamic particle size were quantified and summarized in Table 3. In all formulations, the median particle diameter (D50) was either at or above 5 μm, indicating that the overall geometric particle size was slightly above our target size range for efficient pulmonary delivery to the peripheral lung (38). However, these geometric particle sizes are not expected too substantially hinder inhalation efficiency. The MD (1:3)-40 kDa formulation had the highest D50 value of 8.7 μm with a large span indicating potential agglomeration in the sample. Agglomeration in this sample could also be a consequence of the higher dextran weight fraction, leading to the higher moisture content (Table 3). This presents a concern for inhalation delivery depending on the time scale for aggregation relative to patient administration. Subsequent moisture swell or particle cohesion may have resulted in the higher D50 and broader size distribution found for MD (1:3)-40 kDa. Despite these geometric particle sizes, the MMAD values ranged from 4.4 - 4.9 μm. Based on these results, all formulations have an aerodynamic particle size within the appropriate range of 1-5 μm for delivery to the lungs (39). Since experimental MMAD was smaller than the measured

geometric particle size, these powders can be considered inhalable and are therefore applicable for further study in pulmonary delivery.

3.5 Bulk Powder Flowability

Powder delivery via inhalation must also consider bulk powder properties like bulk density and Carr's Index (Table 2) to develop a successful powder delivery system. A slightly lower bulk density was observed in all formulations containing less mannitol, when testing in low ambient humidity. Lower bulk density in formulations with a 1:3 mannitol-to-dextran implies that there could be less interparticle contact and therefore less cohesion within the bulk state (40). Bulk density was also used to calculate Carr's Index, to assess powder compressibility and flowability. Carr's Index values for each formulation were all above 47, indicating that these formulations produce highly compressible powders (41) and likely possess very poor bulk flow. Ideal powder flowability typically yields Carr's Index values less than 10, while very, very poor flow is represented by values 38 and above (42). While this may primarily be an artifact of the small size of our particles, the relative comparison of Carr's Index values between formulations is still insightful. Of all tested formulations, MD (1:3)-500 kDa was the least compressible and suggests that it would have higher flowability compared to the other powders. In terms of pulmonary powder delivery, the highly compressible nature of this powder requires a delivery method that minimizes powder compression during powder dosage loading. Due to this poor bulk flowability, powder delivery *in vivo* can also benefit from a delivery device that uses positive pressure or physical obstructions to interrupt particle bridging and induce aerosolization.

3.6 Emitted Dose via Intratracheal Delivery

Powder flowability was further analyzed through *in vitro* powder delivery with a hand-held, positive pressure dosator device intended for intratracheal delivery to murine animal models (Figure 1). Figure 5 shows the emitted dose from the custom-made dosator for each mannitol-dextran formulation, as well as the estimated delivered dose that can be sprayed through a 3D printed mouse trachea. Emitted dose was substantially higher in MD (1:3)-500 kDa and MD (3:1)-40 kDa formulations, with 84% and 91% emitted, respectively. The formulations with highest emitted dose also had the lowest Carr's Index values and particle sizes (Tables 2 and 3), predicting better flowability from the dosator tip. The other two formulations, both with a Carr's Index of 53, had significantly lower average emitted doses which were between 40-60%. The wide differences in emitted dose data further supports the claims of others that device performance is highly formulation dependent (28). In all cases, the difference between emitted and delivered dose can be attributed to the larger particles or clumps that became stuck within the 3D printed trachea, representing the dose fraction unlikely to reach the lower airways. It should be noted that relative humidity during device testing was below 25% RH, allowing for relatively high emitted doses. Since the formulations with higher dextran content tend to absorb more moisture, it is expected that emitted dose would be far lower under elevated humidity conditions (43). Based on the high viral loading used in our formulations, a delivered powder mass between 2-4 mg should be sufficient for generating an immune response in mice, provided that viral activity remains high after spray drying (15). With low viral log loss and a high delivered dose above 55%, the MD (1:3)-500 kDa formulation displayed sufficient viral potency within a desired powder mass for successful *in vivo* pulmonary delivery.

4. Conclusions

Within this study, we have demonstrated how excipient ratio and molecular weight within a spray dried formulation impact particle drying dynamics and pulmonary delivery. Incorporating higher molecular weight dextran at a higher mass ratio within a spray dried mannitol-dextran blend can greatly improve retained viral activity in a thermally stable and inhalable dry powder. Increasing the dextran content relative to mannitol caused an increase in viscosity during droplet drying to limit molecular diffusion for more effective encapsulation of the viral vector within the particle core. Adding less mannitol to the blend also reduced crystal exclusion of the labile AdHu5 vector towards an air-solid interface, minimizing viral exposure to thermal stresses.

Formulations with a higher dextran ratio do have a higher capacity for moisture absorption and particle agglomeration, leading to possible challenges with powder delivery within environments of increased humidity and *in vivo* targeting at the lung. Under low humidity conditions (<25% RH), an emitted dose above 84% can be achieved using a custom made intratracheal dosator device that minimizes powder compression. MD (1:3)-500 kDa was the best performing formulation as it minimized processing and aging losses, while also offering suitable particle size and flowability to achieve a high emitted dose for intratracheal delivery. Overall, we have demonstrated that this mannitol-dextran spray dried formulation can maintain high viral potency and strong aerosolization potential, making it a promising candidate for *in vivo* pulmonary vaccine delivery. Since a mannitol-dextran formulation has yet to be granted regulatory approval for inhalation applications, extensive clinical evaluation is still required prior to commercial use.

5. Acknowledgements

The authors would like to thank James Mayo for conducting TGA for moisture analysis, Varsha Singh for training and assistance with particle sizing, Marcia Reid for SEM training and the Canadian Center for Electron Microscopy for use of their imaging facility. We also thank Mark MacKenzie for assisting with 3D printing. We would also like to acknowledge Iconovo for generously providing the ICOone inhalers used in this study.

6. Funding Statement

Funding for this work was provided by the Natural Sciences and Engineering Research Council of Canada (NSERC) and the Canadian Institutes of Health Research (CIHR).

7. Conflict of Interest Statement

The authors of this work declare that they have no conflicts of interest.

8. References

1. Ashok A, Brison M, LeTallec Y. Improving cold chain systems: Challenges and solutions. Vaccine [Internet]. 2017;35:2217–23. Available from: http://dx.doi.org/10.1016/j.vaccine.2016.08.045
2. Comes T, Bergtora Sandvik K, Van de Walle B. Cold chains, interrupted: The use of technology and information for decisions that keep humanitarian vaccines cool. J Humanit Logist Supply Chain Manag. 2018;8(1):49–69.
3. Saluja V, Amorij JP, Kapteyn JC, de Boer AH, Frijlink HW, Hinrichs WLJ. A comparison between spray drying and spray freeze drying to produce an influenza subunit vaccine powder for inhalation. J Control Release. 2010;144(2):127–33.
4. Saboo S, Tumban E, Peabody J, Wafula D, Peabody DS, Chackerian B, et al. Optimized Formulation of a Thermostable Spray-Dried Virus-Like Particle Vaccine against Human Papillomavirus. Mol Pharm. 2016;13(5):1646–55.
5. Ohtake S, Martin RA, Yee L, Chen D, Kristensen DD, Lechuga-Ballesteros D, et al. Heat-stable measles vaccine produced by spray drying. Vaccine. 2010;28:1275–84.
6. Afkhami S, LeClair DA, Haddadi S, Lai R, Toniolo SP, Ertl HC, et al. Spray dried human

and chimpanzee adenoviral-vectored vaccines are thermally stable and immunogenic in vivo. Vaccine [Internet]. 2017;35(22):2916–24. Available from: http://dx.doi.org/10.1016/j.vaccine.2017.04.026

7. Toniolo SP, Afkhami S, D'Agostino MR, Lichty BD, Cranston ED, Xing Z, et al. Spray dried VSV-vectored vaccine is thermally stable and immunologically active in vivo. Sci Rep [Internet]. 2020;10:1–8. Available from: https://doi.org/10.1038/s41598-020-70325-2

8. Crowe JH, Crowe LM, Carpenter JF, Aurell Wistrom C. Stabilization of dry phospholipid bilayers and proteins by sugars. Biochem J. 1987;242(1):1–10.

9. Toniolo SP, Afkhami S, Mahmood A, Fradin C, Lichty BD, Miller MS, et al. Excipient selection for thermally stable enveloped and non-enveloped viral vaccine platforms in dry powders. Int J Pharm [Internet]. 2019;561:66–73. Available from: https://doi.org/10.1016/j.ijpharm.2019.02.035

10. Jeyanathan M, Afkhami S, Smaill F, Miller MS, Lichty BD, Xing Z. Immunological considerations for COVID-19 vaccine strategies. Nat Rev Immunol [Internet]. 2020;20(10):615–32. Available from: http://dx.doi.org/10.1038/s41577-020-00434-6

11. Smaill F, Jeyanathan M, Smieja M, Medina MF, Thanthrige-Don N, Zganiacz A, et al. A human type 5 adenovirus-based tuberculosis vaccine induces robust T cell responses in humans despite preexisting anti-adenovirus immunity. Sci Transl Med. 2013;5(205).

12. Pereira HG, Valentine RC, Russel WC. The Effect of Heat on the Anatomy of the Adenovirus. J genVirol. 1967;1:509–22.

13. Rexroad J, Wiethoff CM, Green AP, Kierstead TD, Scott MO, Middaugh CR. Structural stability of adenovirus type 5. J Pharm Sci. 2003;92(3):665–78.

14. Leclair DA, Cranston ED, Xing Z, Thompson MR. Evaluation of excipients for enhanced thermal stabilization of a human type 5 adenoviral vector through spray drying. Int J Pharm [Internet]. 2016;506:289–301. Available from: http://dx.doi.org/10.1016/j.ijpharm.2016.04.067

15. Manser MM, Feng X, Xing Z, Cranston ED, Thompson MR. Cryoprotective agents influence viral dosage and thermal stability of inhalable dry powder vaccines. Int J Pharm [Internet]. 2022;617(December 2021):121602. Available from: https://doi.org/10.1016/j.ijpharm.2022.121602

16. LeClair DA, Cranston ED, Xing Z, Thompson MR. Optimization of Spray Drying Conditions for Yield, Particle Size and Biological Activity of Thermally Stable Viral Vectors. Pharm Res [Internet]. 2016;33:2763–76. Available from: http://dx.doi.org/10.1007/s11095-016-2003-4

17. Morgan BA, Niinivaara E, Xing Z, Thompson MR, Cranston ED. Validation of a diffusion-based single droplet drying model for encapsulation of a viral-vectored vaccine using an acoustic levitator. Int J Pharm [Internet]. 2021;605(June):120806. Available from: https://doi.org/10.1016/j.ijpharm.2021.120806

18. Tong HHY, Wong SYS, Law MWL, Chu KKW, Chow AHL. Anti-hygroscopic effect of dextrans in herbal formulations. Int J Pharm. 2008;363(1–2):99–105.

19. Galdiero F. Archives of Virology Adenovirus Aggregation and Preservation in Extracellular Environment. Arch Virol. 1979;59:99–105.

20. Kawaizumi F, Nishio N, Nomura H, Miyahara Y. Calorimetric and compressibility study of aqueous solutions of dextran with special reference to hydration and structural change of water. Polym J. 1981;13(3):209–13.

21. Odziomek M, Sosnowski TR, Gradoń L. Conception, preparation and properties of functional carrier particles for pulmonary drug delivery. Int J Pharm. 2012;433(1–2):51–9.

22. Weers JG, Tarara TE, Clark AR. Design of fine particles for pulmonary drug delivery. Expert Opin Drug Deliv. 2007;4(3):297–313.

23. Morgan BA, Xing Z, Cranston ED, Thompson MR. Acoustic levitation as a screening method for excipient selection in the development of dry powder vaccines. Int J Pharm [Internet]. 2019;563:71–8. Available from: https://doi.org/10.1016/j.ijpharm.2019.03.026

24. Lastow O, Arvidsson L. Single Dose Dry Powder Inhaler. EP; EP 3 302 661 B1, 2020.

25. World Health Organization. Bulk density and tapped density of powders. In: The International Pharmacopoeia, Tenth Edition [Internet]. Geneva; 2020. Available from: https://digicollections.net/phint/2020/index.html#d/b.10.4.1

26. Hughes H, Leane MM, Tobyn M, Gamble JF, Munoz S, Musembi P. Development of a Material Sparing Bulk Density Test Comparable to a Standard USP Method for Use in Early Development of API's. AAPS PharmSciTech. 2014;16(1):165–70.

27. Ihara D, Hattori N, Horimasu Y, Masuda T, Nakashima T, Senoo T, et al. Histological Quantification of Gene Silencing by Intratracheal Administration of Dry Powdered Small-Interfering RNA/Chitosan Complexes in the Murine Lung. Pharm Res. 2015;32(12):3877–85.

28. Qiu Y, Liao Q, Chow MYT, Lam JKW. Intratracheal administration of dry powder formulation in mice. J Vis Exp. 2020;2020(161):1–12.

29. Masaro L, Zhu XX. Physical models of diffusion for polymer solutions, gels and solids. Vol. 24, Progress in Polymer Science (Oxford). 1999. 731–775 p.

30. Mazzarotta A, Caputo TM, Raiola L, Battista E, Netti PA, Causa F. Small oligonucleotides detection in three-dimensional polymer network of dna-peg hydrogels. Gels. 2021;7(3):1–16.

31. Meerdink G, van't Riet K. Modeling segregation of solute material during drying of liquid foods. AIChE J. 1995;41(3):732–6.

32. Kadota K, Yanagawa Y, Tachikawa T, Deki Y, Uchiyama H, Shirakawa Y, et al. Development of porous particles using dextran as an excipient for enhanced deep lung delivery of rifampicin. Int J Pharm [Internet]. 2019;555(May 2018):280–90. Available from: https://doi.org/10.1016/j.ijpharm.2018.11.055

33. Larsen BS, Skytte J, Svagan AJ, Meng-Lund H, Grohganz H, Löbmann K. Using dextran of different molecular weights to achieve faster freeze-drying and improved storage

stability of lactate dehydrogenase. Pharm Dev Technol [Internet]. 2019;24(3):323–8. Available from: https://doi.org/10.1080/10837450.2018.1479866

34. Palomäki E, Ahvenainen P, Ehlers H, Svedström K, Huotari S, Yliruusi J. Monitoring the recrystallisation of amorphous xylitol using Raman spectroscopy and wide-angle X-ray scattering. Int J Pharm. 2016;508(1–2):71–82.

35. Yu L, Mishra DS, Rigsbee DR. Determination of the glass properties of D-mannitol using sorbitol as an impurity. J Pharm Sci. 1998;87(6):774–7.

36. Hubálek Z. Protectants used in the cryopreservation of microorganisms. Cryobiology. 2003;46:205–29.

37. Prudic A, Ji Y, Luebbert C, Sadowski G. Influence of humidity on the phase behavior of API/polymer formulations. Eur J Pharm Biopharm [Internet]. 2015;94:352–62. Available from: http://dx.doi.org/10.1016/j.ejpb.2015.06.009

38. Chaurasiya B, Zhao YY. Dry powder for pulmonary delivery: A comprehensive review. Pharmaceutics. 2021;13(1):1–28.

39. Darquenne C. Aerosol deposition in health and disease. J Aerosol Med Pulm Drug Deliv. 2012;25(3):140–7.

40. Aulton ME. Part 2: Particle Science and Powder Technology - Powder Flow. In: Aulton ME, Taylor KMG, editors. Aulton's Pharmaceutics: The Design and Manufacture of Medicines. Fifth Edit. 2018. p. 189–92.

41. Sarraguça MC, Cruz A V., Soares SO, Amaral HR, Costa PC, Lopes JA. Determination of flow properties of pharmaceutical powders by near infrared spectroscopy. J Pharm Biomed Anal. 2010;52(4):484–92.

42. Turchiuli C, Fuchs M, Bohin M, Cuvelier ME, Ordonnaud C, Peyrat-Maillard MN, et al. Oil encapsulation by spray drying and fluidised bed agglomeration. Innov Food Sci Emerg Technol. 2005;6(1):29–35.

43. Kwok PCL, Chan HK. Effect of relative humidity on the electrostatic charge properties of dry powder inhaler aerosols. Pharm Res. 2008;25(2):277–88.

44. Rahman MS, Al-Marhubi IM, Al-Mahrouqi A. Measurement of glass transition temperature by mechanical (DMTA), thermal (DSC and MDSC), water diffusion and density methods: A comparison study. Chem. Phys. Lett. 2007;440(4):372-377.

45. Newman A, Zografi G. Commentary: Considerations in the Measurement of Glass Transition Temperatures of Pharmaceutical Amorphous Solids. AAPS PharmSciTech. 2020;21(1):1-13.

46. Brandau DT, Jones LS, Wiethoff CM, Rexroad J, Middaugh CR. Thermal stability of vaccines. J Pharm Sci. 2003;92(2):218–31.

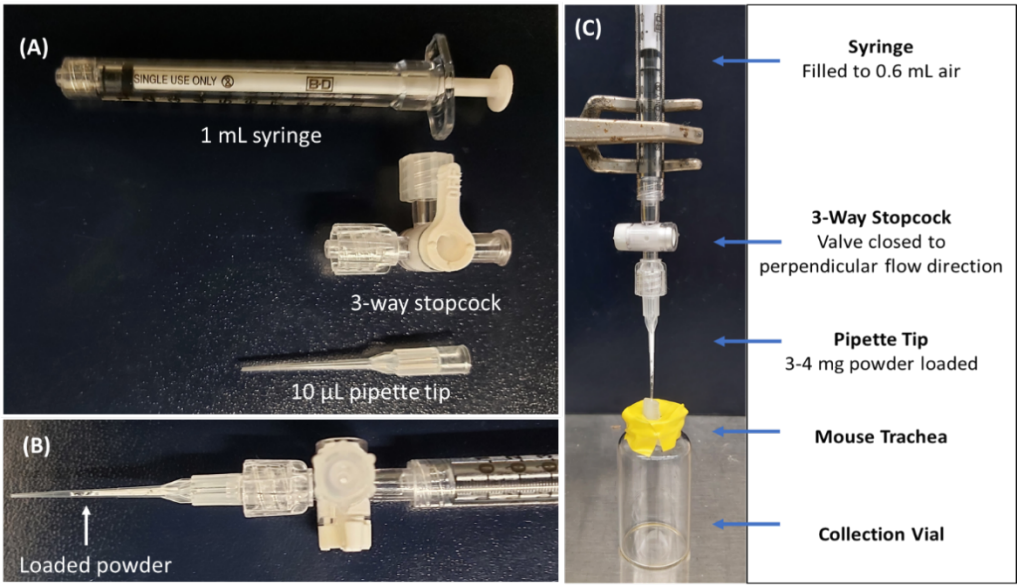

Figure 1. Custom made intratracheal dosator intended for *in vivo* delivery to mice using assembled components (Panel A) including: a 1 mL syringe with luer lock connection, 3-way stopcock and a 10 µL pipette tip. Spray dried powder is loaded into the pipette tip and all components are assembled tightly together (Panel B). A full experimental set up is pictured in Panel C, showing the syringe, dosator assembly, 3D mouse trachea model and a powder collection vial.

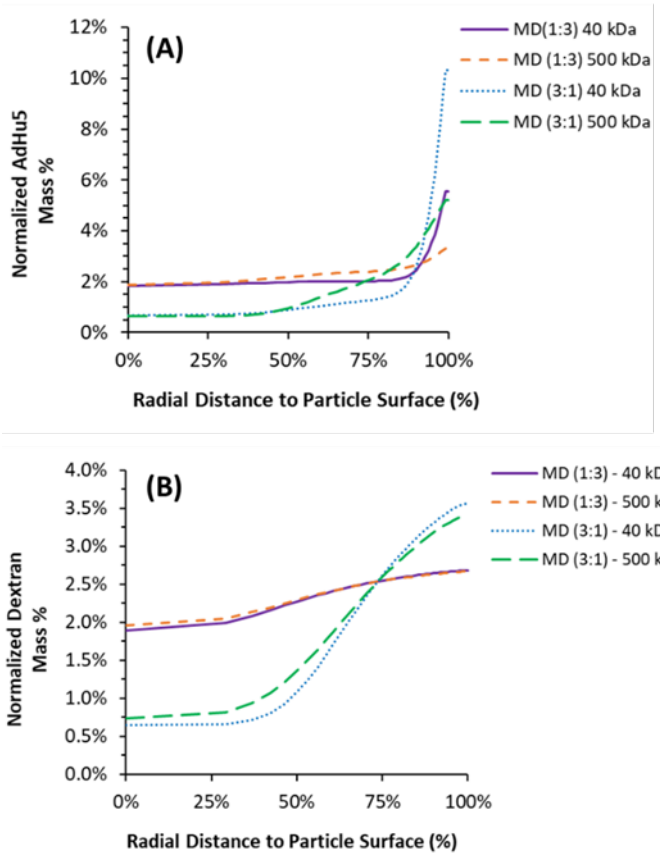

Figure 2. Model predicted, normalized mass distribution of (A) AdHu5 adenoviral vector and (B) dextran within a mannitol-dextran particle. Radial distance refers to the percentage of distance between the particle core (0%) and the particle surface (100%). Mass% of each component was normalized based on the total amount of that component added to the formulation. Excipient formulations include mannitol and dextran in a ratio by mass of either 1:3 or 3:1, respectively, and a dextran molecular weight of either 40 kDa or 500 kDa.

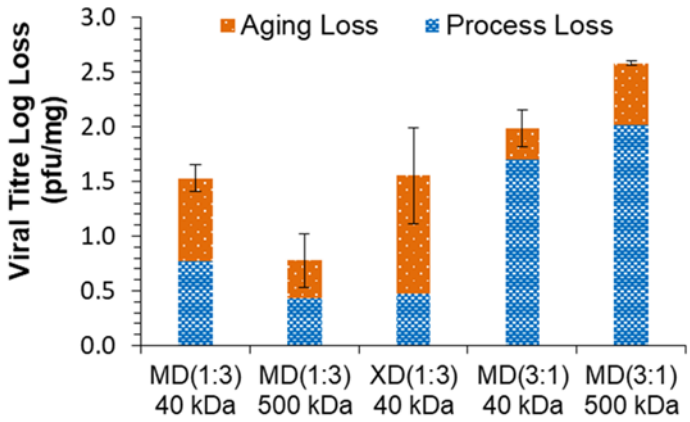

745

Figure 3. Viral titre log loss (pfu/mg) of spray dried AdHu5 adenoviral vector with excipient formulations using mannitol with dextran (MD) in a ratio by weight of either 1:3 or 3:1 and either a low molecular weight dextran (40 kDa) or high molecular weight dextran (500 kDa). A xylitol-dextran (XD) formulation with a 1:3 ratio using 40 kDa dextran is also shown. Process loss refers
750 to viral titre loss from spray drying compared to the stock viral titre, while aging losses are associated with the additional viral titre loss after samples were stored at 45ºC for 72 hours prior to in vitro testing. All samples were tested in duplicate and error bars represent the resulting standard error.

755

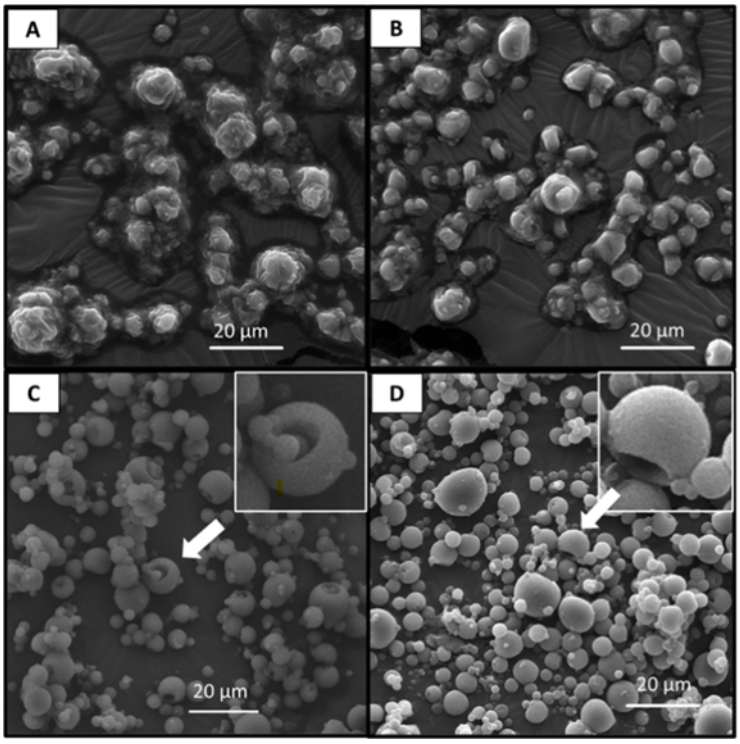

760

Figure 4. Scanning electron microscope (SEM) images showing particle morphology of the following mannitol-dextran (MD) spray dried powders: (A) MD (1:3)–40 kDa dextran, (B) MD (1:3)–500 kDa dextran (C) MD (3:1)–40 kDa dextran and (D) MD (3:1)–500 kDa dextran. Arrows indicate particle dimpling and indentation likely due to hollow shell formation. All images were
765 captured at 2000 X magnification with a scale bar representing 20 µm in length.

770

775

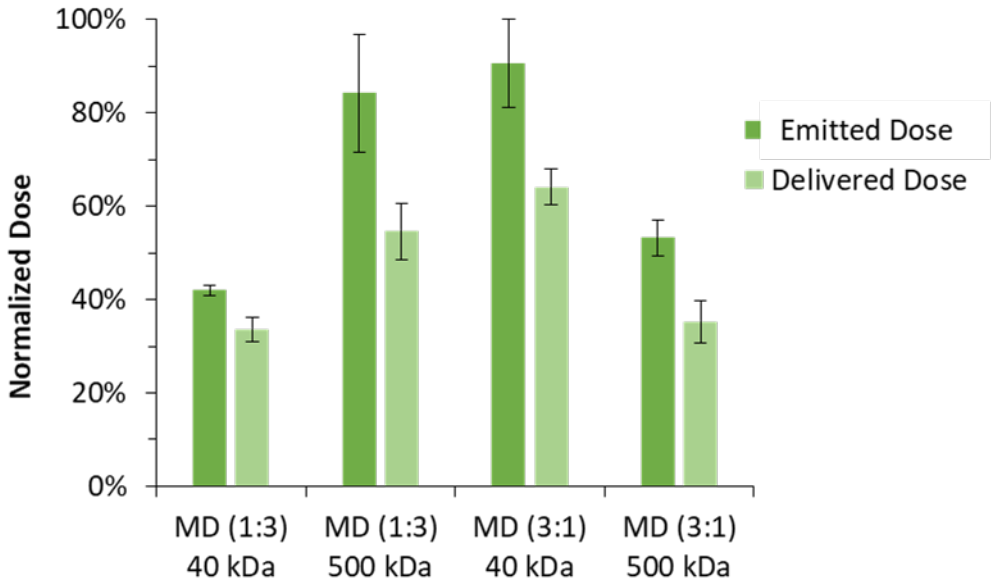

Figure 5. Normalized dose of spray dried powder dispersed from custom made dosator device (Figure 1), for each respective mannitol-dextran formulation in a ratio by weight of either 1:3 or 3:1 using a low molecular weight dextran (40 kDa) or high molecular weight dextran (500 kDa). Emitted dose refers to the powder dosage exiting the needle tip of the dosator upon actuation. Delivered dose represents the percentage of powder collected after powder was sprayed from the dosator and directly through a 3D printed mouse trachea, mimicking endotracheal delivery. Both emitted and delivered dose were normalized based on powder mass initially loaded. Error bars represent standard error between replicate measurements (n=3).